International Journal of Mass Spectrometry 294 (2010) 88–92

Contents lists available at ScienceDirect

International Journal of Mass Spectrometry

journal homepage: www.elsevier.com/locate/ijms

Dissociation dynamics of energy-selected acetic acid ions: The gas phase heat of formation of the acetyl ion

Nicholas S. Shuman[1], William R. Stevens[2], Tomas Baer*

Department of Chemistry, The University of North Carolina at Chapel Hill, Chapel Hill, NC 27599-3290, USA

ARTICLE INFO

Article history:
Received 29 March 2010
Received in revised form 13 May 2010
Accepted 20 May 2010
Available online 27 May 2010

Keywords:
TPEPICO
Dissociation onset
Statistical theory
Acetic acid
Acetyl ion
Heat of formation

ABSTRACT

The dissociation of energy-selected acetic acid ions (CH_3COOH^+) has been investigated by Threshold Photoelectron–photoion Coincidence (TPEPICO) spectroscopy. The lowest energy dissociation pathway for CH_3COOH^+ is $OH^\bullet$ loss, and the 0 K onset (E_0) of this process is measured to be 11.641 ± 0.008 eV. The reaction rate for this step is instantaneous on the time-scale of the experiment so that no rate theory is required to extract its onset. Because the heats of formation of acetic acid and the $OH^\bullet$ radical are known to an accuracy of ±0.5 kJ/mol, we can use the $OH^\bullet$ loss onset to obtain an accurate heat of formation of the acetyl ion, $\Delta_f H^\circ_{298\,K}[CH_3CO^+] = 658.5 \pm 1.0$ kJ/mol, which agrees to within 0.9 kJ/mol with an earlier determination based on $CH_3^\bullet$ loss from the acetone ion. At higher energies, the acetic acid ion loses $CH_3^\bullet$ to form the $HOCO^+$ ion in competition with the lower energy OH-loss. Two versions of the statistical reaction rate theory failed to reproduce the branching ratios for these higher energy parallel reactions. Because of the magnitude of this disagreement, we conclude that the acetic ion may dissociate non-statistically at these higher energies.

1. Introduction

The thermochemistry of small organic molecules has been revolutionized in recent years by experimental and theoretical advances, so that accuracies of ±1 kJ/mol, or better, are not unusual [1–5]. A major impetus in this process has been the development of the active thermochemical tables (ATcT) [6], which recognizes that a single thermochemical experiment only measures differences between the heats of formation of any two species, and that a variety of experiments measuring the same quantity via multiple paths are the key to establishing accurate numbers. The dissociative photoionization of acetic acid to produce acetyl, CH_3CO^+, as well as $HOCO^+$ ions, are good examples of reactions that connect important chemical species, whose accurate energy difference measurements would improve the heats of formation of all species involved.

The dissociative photoionization of acetic acid to produce the acetyl ion and $OH^\bullet$ has been reported by Traeger et al. [7] using photoionization mass spectrometry in which the dissociation energy is determined by using a linear extrapolation of the fragment ion signal to the baseline. They reported an onset of 11.54 eV with no error bars, and used this value, among others, to derive a heat of formation of the acetyl ion. Because there is no a priori correct extrapolation, such onsets are often unreliable. Here we measure the onset using threshold photoelectron–photoion coincidence (TPEPICO) spectroscopy, a technique that yields sharper onsets because signal as a function of the photon energy is essentially the derivative of the photoionization scan. Equally important is the fact that TPEPICO explicitly accounts for the thermal energy distribution of the dissociating neutral, allowing for determination of the onset to within 1 kJ/mol (0.01 eV). Thermochemistry is extracted by relating the 0 K onset energy to the difference between the product and reactant 0 K heats of formation, as shown in Eq. (1)

$$E_0 = \Delta_f H^\circ_{0\,K}[CH_3CO^+] + \Delta_f H^\circ_{0\,K}[OH^\bullet] - \Delta_f H^\circ_{0\,K}[CH_3COOH] \quad (1)$$

In this equation, all three species have reasonably well established heats of formation. The $OH^\bullet$ radical was last updated in 2002 by Ruscic et al. [8] where $\Delta_f H^\circ_{0\,K}[OH^\bullet]$ is listed as 37.0 ± 0.3 kJ/mol. The acetic acid 298 K heat of formation in its liquid state is listed as −484.3 ± 0.2 kJ/mol by Pedley [9]. The same Pedley compilation lists the vapor phase heat of formation with an error of ±2.5 kJ/mol because of the poorly known heat of vaporization. However, the heat of vaporization was remeasured by Verevkin [10] in 2000 so that the 298 K heat of formation of acetic acid vapor is −434.1 ± 0.5 kJ/mol. The least well known heat of formation is that of the acetyl ion, whose 0 K value was last reported in 2005 to be 666.7 ± 1.1 kJ/mol by Fogleman et al. [11] based on the dissocia-

* Corresponding author. Tel.: +1 919 962 1580; fax: +1 919 962 2388.
E-mail address: baer@unc.edu (T. Baer).
[1] Current address: Air Force Research Laboratory, Space Vehicles Directorate, 29 Randolph Rd., Hanscom Air Force Base, Massachusetts 01731-3010, USA.
[2] Current address: U.S. Environmental Protection Agency, Office of Research and Development, E305-01, 109 T.W. Alexander Drive, Research Triangle Park, NC 27711, USA.

1387-3806/$ – see front matter © 2010 Elsevier B.V. All rights reserved.
doi:10.1016/j.ijms.2010.05.021

tive photoionization of acetone using the TPEPICO technique. OH• loss from acetic acid ions thus provides us with another route to the acetyl ion heat of formation. This is quite welcome since the acetone ion dissociation is made complicated by a lower energy CH_4 loss channel.

Determining the higher energy $HOCO^+$ onset requires careful modeling of the rate-energy ($k(E)$) curves of both CH_3CO^+ and $HOCO^+$ formation [12]. For homolytic bond cleavages this is not trivial. In such dissociations, the geometry and vibrational frequencies of the transition state, and therefore the $k(E)$, are dependent upon the internal energy of the ion. Statistical rate theories differ on how this energy dependence is treated. The statistical adiabatic channel model (SACM) [13,14] and variational transition state theory (VTST) [15,16] account for this energy dependence rigorously but are not tractable for the dissociations of larger molecules. Simplified versions of these theories have been proposed [17,18] but there is a dearth of systems with known onsets that can be used to test these simplified theories. The onset for $HOCO^+$ formation can be determined to within 2 kJ mol^{-1} from literature heats of formation, thus providing an opportunity to test different statistical theories for modeling higher energy onsets.

2. Experimental method

The TPEPICO methodology has been described in great detail elsewhere [19–21]. Sample vapor is introduced into a vacuum chamber through a temperature controlled inlet, and ionized by vacuum ultraviolet (VUV) radiation from a molecular hydrogen lamp dispersed by a 1 m normal incidence monochromator (photon resolution about 8 meV at 10 eV). The ionization event produces electrons and ions which are accelerated in opposite directions by an electric field of 20 V cm^{-1}. Electrons are velocity map focused, such that electrons with no velocity perpendicular to the acceleration axis are collected by a Channeltron electron multiplier masked by a 1.4 mm diameter aperture. This will include both threshold (zero kinetic energy) electrons and energetic electrons with velocity directed only along the acceleration axis. The contribution of energetic electrons is accounted for by also collecting electrons with an off-axis Channletron detector masked by a 2 mm × 6 mm rectangular aperture. Because electrons from large molecules such as acetic acid are produced quasi-isotropically, the number of on-axis energetic electrons detected is proportional to the off-axis signal, and can be subtracted from the on-axis signal. The remaining on-axis signal consists solely of events producing energy-selected ions, in that the internal energy of each ion is defined by the incident photon energy and the initial thermal energy of the neutral. Upon extraction from the first acceleration region, ions are accelerated once more to a kinetic energy of 250 V and travel through a field free region of 40 cm before detection by a multi channel plate detector. Time-of-flight (TOF) spectra are produced by measuring the time between electron and ion detection. The relative peak areas in these TOF spectra are proportional to the product ion branching ratios resulting from the photoionization of acetic acid neutrals with a well-defined initial energy distribution. In order to account for the gas phase dimer concentration, the data were collected at several temperatures, up to 355 K.

3. Results and analysis

A series of time-of-flight (TOF) mass spectra were collected for energy-selected ions at various photon energies from below to well above the dissociation limits for OH• and CH_3• loss. These data are summarized in the breakdown diagram (Fig. 1) which shows the fractional parent and product ion abundances plotted as a function of photon energy. The rise and fall of the ion abundances show that the lowest energy dissociation channels are

$$CH_3COOH^+ \rightarrow CH_3CO^+ + OH^\bullet \quad (2)$$

$$CH_3COOH^+ \rightarrow HOCO^+ + CH_3^\bullet \quad (3)$$

where OH• loss is the lowest energy pathway. Based on the symmetric fragment ion TOF distributions, we know that the acetic acid ion dissociation occurs fast on the time-scale of our experiment (the apparatus is able to measure dissociation rate constants up to 10^7 s^{-1}, setting a lower limit for this reaction at threshold). That is, any parent ion with a sufficient internal energy, $E_{int} = h\nu + E_{thermal}$, to dissociate will do so prior to entering the 40 cm field free region. As a result, the observed relative acetic acid parent and fragment ion abundances are simply a function of the 0 K onset and the initial thermal energy distribution of the ions. Several experiments have shown that the ion thermal energy distribution is well described by simply transposing the neutral thermal energy distribution up to the ionic manifold [21,22]. After accounting for the finite photon resolution, the lowest energy 0 K onset is clearly identified by

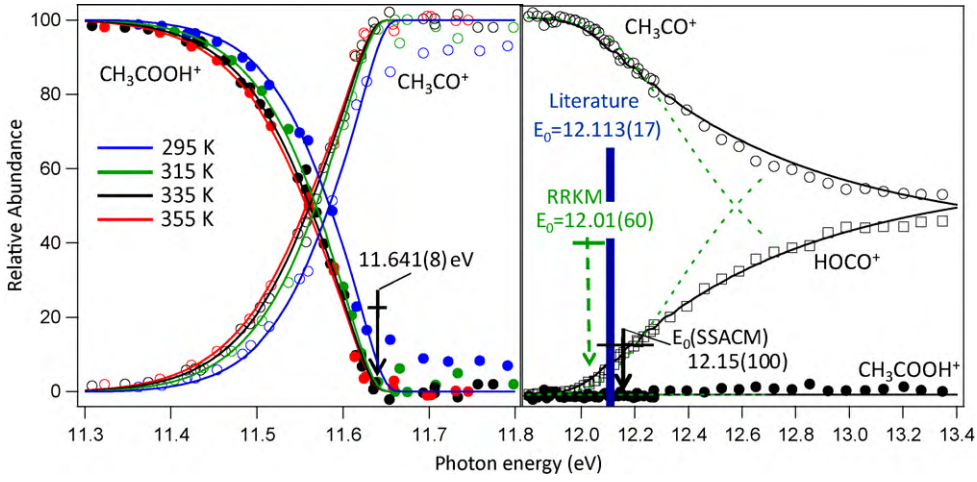

Fig. 1. (a) Breakdown diagrams of acetic acid taken at the indicated temperatures. The best-fit curves are independent of the dissociation rate (see text). Onset shown is an average value excluding the 295 K data; the value in parentheses is the uncertainty in meV. (b) Breakdown diagram of acetic acid in the energy range of $HOCO^+$ formation at 355 K. The Best-fit curves were modeled using either RRKM (dashed green lines) or SSACM (solid black lines) assuming no isomerization to the enol ion. The "good" fit of SSACM involves an unphysical "c" parameter (see text). Arrows indicate 0 K onsets using each model; the width of the vertical blue bar indicates the uncertainty in the literature onset. Note the change in horizontal scale between (a) and (b). (For interpretation of the references to color in this figure legend, the reader is referred to the web version of the article.).

the photon energy at which the parent ion abundance reaches zero. Determining the higher energy CH_3• loss onset is more complicated because it requires modeling the relative rates of the competing channels, and we will return to this point below.

4. The OH• loss onset

The identification of the lowest energy onset from acetic acid is complicated by the presence of acetic acid dimers. At room temperature, peaks corresponding to both the protonated acetic acid monomer and methyl-loss from the acetic acid dimer were observed in the mass spectrum, in agreement with previous work [23]. Ideally, the dimer/monomer equilibrium could be measured as a function of sample temperature by comparing the dimer and monomer peaks in the mass spectrum. However, the acetic acid dimer is never seen in the mass spectrum, suggesting that any dimer ions immediately dissociate. We note that while the dimer ion is a bound species (by roughly 100 kJ mol^{-1} relative to the observed dissociation channels as calculated using the G3 [24] model chemistry), its equilibrium geometry is very different from that of the neutral dimer, and the neutral dimers must be vertically excited to a repulsive portion of the dimer ion potential. The dimer contribution to the mass spectrum is monitored by the relative abundance of the peaks in the mass spectrum that can only originate from the dimer, namely the peaks at m/z 61 and 115. Fig. 2 shows portions of the TOF mass spectra at identical photon energies taken at room temperature and at 335 K. In the room temperature spectrum, the peak at m/z 61 (the protonated monomer) is evident with an abundance well above the 2% of the m/z 60 peak that would be expected from $^{13}CH_3COOH$. At 335 K, the m/z 61 peak is entirely reduced to the expected 2% isotope peak. It is worth noting that the m/z 60 peak has a form that can be modeled with two Gaussian functions of different widths. The reason for this is that our sample is introduced by a hypodermic needle which causes a portion of the molecules to have a low velocity in the direction of the ion extraction, whereas the rest of the molecules have a 3-D Maxwell Boltzmann translational energy distribution caused by wall collisions.

While no significant amount of the protonated monomer ion is produced at 335 K, it is still possible that the dimer ions preferentially dissociate to the monomer ion. If this were the case, then the photon energy at which the m/z 60 ion abundance reached zero would be a function of the acetic acid monomer/dimer equilibrium populations and would change with sample temperature. Breakdown diagrams were taken at several temperatures (295 K, 315 K, 335 K, and 355 K). As shown in Fig. 1, the m/z 60 abundance at room temperature remains elevated at higher photon energies compared to the higher temperature data. At 315 K the m/z 60 ion abundance reaches zero at 11.645 eV, an almost identical onset as that seen in the higher temperature breakdowns. If monomer ions were being produced from dissociated dimer at these temperatures in any significant amount, the onset would continue to shift to lower energies as the temperature increased. It is perhaps not surprising that the dimer ion does not dissociate to the monomer ion. Rather, we should view the nascent "dimer ion" as a collision complex between an acetic acid ion and its monomer, which yields the more stable protonated monomer ion as a product. According to data on the NIST Webbook [25] and the bond dissociation energy of CH_3COO–H found in Luo [26], the protonated acetic acid product is more stable by 14 kJ/mol than the monomer ion.

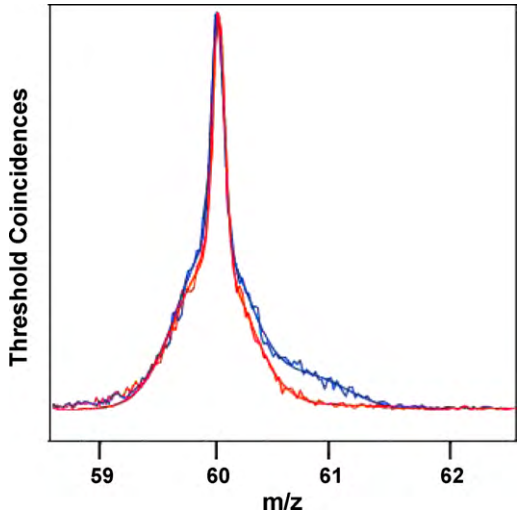

Fig. 2. TOF spectra of acetic acid at 295 K (blue) and 335 K (red). Curves shown are summations of three Gaussians used to describe the expected curve shapes of the narrow jet peak and broad thermal peak comprising the parent signal at m/z 60 and the broad peak of the daughter ion at m/z 61. (For interpretation of the references to color in this figure legend, the reader is referred to the web version of the article.).

Table 1
Heats of formation derived and used in this study.

Species	$\Delta H^\circ_{f,0\,K}$	$H_{298-0\,K}$	$\Delta H^\circ_{f,298\,K}$
CH_3COOH	−420.4 ± 0.5[a]	14.0	−434.1 ± 0.5[b]
$HOCO^+$	600.3 ± 1[c]	11.0	597.3 ± 1[c]
CH_3CO^+	665.8 ± 1.0[d]	11.8	658.5 ± 1.0[d]
	666.7 ± 1.1[e]		659.4 ± 1.1[e]
OH•	37.0 ± 0.3[f]		37.3 ± 0.3[f]
CH_3•	150.0 ± 0.3[g]	10.37	146.7 ± 0.3[g]

[a] Converted from 298 K value based on the experimental CH_3COOH frequencies from Shimanouchi [36].
[b] Pedley [9] and Verevkin [10].
[c] Shuman et al.[32].
[d] This work.
[e] Fogleman et al. [11].
[f] Ruscic et al. [8].
[g] Ruscic et al. [3].

It is known that acetic acid ions may isomerize to the enol [27]. Calculations by Heinrich and Schwarz [27] suggested that the barrier for isomerization lies ~225 kJ mol^{-1} above the ground state ion, far above the observed onset to OH• loss (≈95 kJ mol^{-}). Our own G3 calculations indicate that the barrier is only about 105 kJ/mol above the acetic acid ion ground state, so that isomerization could intervene. However, if the isomerization occurs, it proceeds rapidly as all ions are seen to dissociate through OH-loss with a rate constant greater than 10^7 s^{-1}, and the observed onset still indicates the threshold production of channel 1. The 0 K onset of 11.641 ± 0.008 eV for reaction (1) is taken as the average of the highest temperature breakdown diagrams. Excluding the room temperature data, all the onsets agree to within 2 meV, well within the uncertainty of the measurements. This can be compared to the Traeger onset of 11.54 eV, which is obtained by extrapolating the photoion signal to the background. In the absence of variable temperature studies [28], it is common to convert such onsets to 0 K onsets by adding the acetic acid thermal energy (vibrations and rotations) to this onset, which yields a 0 K onset of 11.63 eV, which is within 10 meV of our result. The derived thermochemistry is shown in Table 1 and discussed below.

5. The CH_3• loss onset

The onset for the CH_3• loss reaction is much more difficult to determine from the data. While the breakdown diagram below the second onset is independent of the dissociation rate, above the onset the breakdown diagram reflects the relative rates of the parallel dissociation channels. Unfortunately, the experiment gives no information about the absolute rate of dissociation, other than that

at threshold the lower energy channel is faster than can be measured with this apparatus. In order to determine the second onset, the rates of both dissociation channels must be modeled.

Unimolecular dissociations that proceed over an energetic maximum along the reaction coordinate have an energy-independent transition state and Rice–Ramsperger–Kassel–Marcus (RRKM) theory may be used to accurately predict the dissociation rate [29]. Both channels here are simple ionic bond cleavages, which typically lack a reverse barrier and therefore a well-defined transition state. While RRKM requires knowledge of only the equilibrium and transition state structures, a rigorous calculation of the specific rate curve for a barrierless dissociation requires knowledge of the potential energy surface along the entire reaction coordinate. Both the Variational Transition State Theory (VTST) [17,30] and the Statistical Adiabatic Channel Model (SACM) [13,14] are examples of such a rigorous approach, however the calculations are arduous at best and intractable at worst. Troe has proposed the Simplified Statistical Adiabatic Channel Model (SSACM), requiring no more effort than RRKM, as an alternative approach [18,31].

The onsets of both $OH^{\bullet}$ and $CH_3^{\bullet}$ loss channels are known because the heats of formation of all relevant species are known. We can therefore use these reaction onsets, along with an acetic acid IE of 10.65 eV, to test the reliability of different statistical theories in extrapolating to the 0 K dissociation onset of the higher energy reaction and comparing to the known literature value of 12.113 ± 0.017 eV. This calculated value is obtained with a new heat of formation of the $HOCO^+$ ion recently calculated by Shuman et al. [32] using the HEAT method [4,33]. This new $\Delta_f H^\circ_{0\,K}[HOCO^+] = 600.3 \pm 1$ kJ/mol is quite close to the previously accepted experimental value (599.1 ± 2 kJ/mol) based on the H loss reaction of formic acid by Ruscic et al. [34].

Surprisingly, neither RRKM nor SSACM properly models the rates of the parallel channels. As shown in the higher energy part of Fig. 1, RRKM overestimates the rate of $CH_3^{\bullet}$ loss relative to the first OH-loss channel at energies above the onset. In previous failures of RRKM in modeling simple bond breaking reactions [18,31], the theory was perfectly capable of fitting the data. Its failure was only in predicting an onset that was too low, which is also the case here. The rapid rise in the RRKM yield for $CH_3^{\bullet}$ loss is due to the extra degree of freedom in the methyl co-product of compared to the $OH^{\bullet}$ co-product of channel 1. Because the isomerization barrier between acetic acid ion and the lower energy enol ion is 1.1 eV, nearly coincident with the higher energy onset, it is possible that the lower energy structure contributes to the density of states of the dissociating species. If this is the case, the rapid rise of the $CH_3^{\bullet}$ loss channel is somewhat mitigated, but RRKM still fails to reproduce the breakdown diagram. SSACM is able to reproduce the breakdown diagram at an onset equal to the literature value within uncertainty, however only by assuming extremely tight transition states (in the language of the model, both channels are fit with very low energy rigidity factors). In this extreme, the transitional modes do not contribute to the transition state sum of states, resulting in unphysical rate curves that are both highly structured and rise unrealistically slowly with the ion internal energy. This is the case whether or not isomerization to the enol ion is considered. We show the perfect fit to the breakdown diagram to illustrate the hazards of using this parameterized rate model without careful reflection about the meaning of the rigidity factor (Ref. [18]).

We thus conclude that neither RRKM nor SSACM is capable of fitting the experimental breakdown diagram. The question is why should these theories break down? Could these parallel dissociation steps be non-statistical? Because of the strong long range forces between the ion and its polarizable neutral, numerous ionic dissociation reactions have been successfully modeled with various versions of the statistical theory. A few reactions, mostly with ions containing F atoms dissociate directly from excited electronic states along a repulsive potential. One example from our laboratory is the direct dissociation of the Br atom from ethyl bromide ions in the first excited electronic state, which manifests itself by a sudden increase in the translational energy release when the ion is prepared in the excited state [35].

Because we do not have any absolute rate information, we cannot provide any direct experimental evidence for non-statistical behavior. However, we note that the RRKM calculated rate curve (which has reasonable transition state vibrational frequencies) indicates that if the reaction were statistical it would rapidly increase to nearly 10^{13} s^{-1} at the $CH_3^{\bullet}$ onset, which is in a regime where the rates of dissociation and flow of vibrational energy are expected to be of the same order of magnitude, thus violating a basic assumption of the statistical theory. In addition, the $CH_3^{\bullet}$ onset lies in the 2nd electronic state. Our model depends upon rapid internal conversion to the ground electronic state, which may or may not take place. Unfortunately, our data do not provide any clues as to why this reaction might be non-statistical.

6. Derived thermochemistry of the acetyl ion

The 0 K onset for $OH^{\bullet}$ loss defines the energy difference between ground state acetic acid and the hydroxyl radical and CH_3CO^+ ion. Because the heats of formation of the both the $OH^{\bullet}$ radical [8] and acetic acid [10] are very well known, the onset can be used to determine a heat of formation of the acetyl ion. The 298 K heat of formation of acetic acid was converted to 0 K using the vibrational frequencies listed in Shimanuchi [36], treating the low frequency mode as a vibration with a frequency of 93 ± 30 cm^{-1}. This uncertainty adds an error to the $H_{298}-H_0$ of only 0.15 kJ/mol. The derived $\Delta_f H^\circ_{0\,K}[CH_3CO^+] = 665.8 \pm 1.0$ kJ/mol, a value in excellent agreement with our previous determination[11] of this quantity of 666.7 ± 1.2 kJ/mol based on the photoionization of acetone. This is gratifying because the $CH_3^{\bullet}$ loss from the acetone ion reaction was complicated by a lower energy CH_4 loss, which had to be accounted for. Confirmation of the acetyl ion heat of formation is important because the most accurate methods of computational thermochemistry [5,37] are now capable of 1 kJ mol^{-1} accuracy, and increasing the pool of experimentally known values with that precision aids in evaluation of the calculated results. Additionally, the active thermochemical tables [2] depend on reliable error bars as well as precise measurements such as this in order to determine a self-consistent network of heats of formation across a wide range of species.

Acknowledgments

The authors are grateful for helpful discussions with Jürgen Troe, and acknowledge the US Department of Energy for financial support of this work.

References

[1] J. Aguilera-Iparraguirre, A.D. Boese, W. Klopper, B. Ruscic, Accurate ab initio computation of thermochemical data for C_3H_x ($x = 0, \ldots, 4$) species, Chem. Phys. 346 (2008) 56–68.
[2] B. Ruscic, R.E. Pinzon, M.L. Morton, G. Laszevski, S.J. Bittner, S.G. Nijsure, K.A. Amin, M. Minkoff, A.F. Wagner, Introduction to active thermochemical tables: several "Key" enthalpies of formation revisited, J. Phys. Chem. A 108 (2004) 9979–9997.
[3] B. Ruscic, J.E. Boggs, A. Burcat, A.G. Császár, J. Demaison, R. Janoschek, J.M.L. Martin, M.L. Morton, M.J. Rossi, J.F. Stanton, P.G. Szalay, P.R. Westmoreland, F. Zabel, T. Berces, IUPAC critical evaluation of thermochemical properties of selected radicals. Part I, J. Phys. Chem. Ref. Data 34 (2005) 573–656.
[4] A. Tajti, P.G. Szalay, A.G. Csaszar, M. Kallay, J. Gauss, E.F. Valeev, B.A. Flowers, J. Vazquez, J.F. Stanton, HEAT: high accuracy extrapolated ab initio thermochemistry, J. Chem. Phys. 121 (2004) 11599–11613.

[5] A. Karton, E. Rabinovich, J.M.L. Martin, B. Ruscic, W4 theory for computational thermochemistry: in pursuit of confident sub-kJ/mol predictions, J. Chem. Phys. 125 (2006), 125144108-1-144108/17.
[6] B. Ruscic, R.E. Pinzon, M.L. Morton, G. Laszevski, S.J. Bittner, S.G. Nijsure, K.A. Amin, M. Minkoff, D. Leahy, D. Montoya, A.F. Wagner, Active thermochemical tables: thermochemistry for the 21st century, J. Phys. Conf. Ser. 16 (2005) 561–570.
[7] J.C. Traeger, R.G. McLoughlin, A.J.C. Nicholson, Heat of formation for acetyl cation in the gas phase, J. Am. Chem. Soc. 104 (1982) 5318–5326.
[8] B. Ruscic, A.F. Wagner, L.B. Harding, R.L. Asher, D. Feller, D.A. Dixon, K.A. Peterson, Y. Song, X.-M. Qian, C.Y. Ng, J. Liu, W. Chen, D.W. Schwenke, On the enthalpy of formation of hydroxyl radical and gas-phase bond dissociation energies of water and hydroxyl, J. Phys. Chem. A 106 (2002) 2727–2747.
[9] J.B. Pedley, Thermochemical Data and Structures of Organic Compounds, Thermodynamics Research Center, College Station, 1994.
[10] S.P. Verevkin, Measurement and prediction of the monocarboxylic acids thermochemical properties, J. Chem. Eng. Data 45 (2000) 953–960.
[11] E.A. Fogleman, H. Koizumi, J.P. Kercher, B. Sztáray, T. Baer, The heats of formation of the acetyl radical and ion obtained by threshold photoelectron photoion coincidence, J. Phys. Chem. A 108 (2004) 5288–5294.
[12] T. Baer, B. Sztáray, J.P. Kercher, A.F. Lago, A. Bodi, C. Scull, D. Palathinkal, Threshold photoelectron photoion coincidence studies of parallel and sequential dissociation reactions, Phys. Chem. Chem. Phys. 7 (2005) 1507–1513.
[13] M. Quack, J. Troe, Specific rate constants of unimolecular processes. II. Adiabatic channel model, Ber. Bunsenges. Phys. Chem. 78 (1974) 240–252.
[14] J. Troe, Statistical adiabatic channel model for ion-molecule processes, J. Chem. Phys. 87 (1987) 2773–2780.
[15] S.J. Klippenstein, R.A. Marcus, Unimolecular rate theory for highly flexible transition states. Use of conventional coordinates, J. Phys. Chem. 92 (1988) 3105–3109.
[16] S.J. Klippenstein, R.A. Marcus, Unimolecular reaction rate theory for highly flexible transition states. 2. Conventional coordinate formulas for various possible fragment combintaions. Miscellaneous topics, J. Phys. Chem. 92 (1988) 5412–5417.
[17] W.J. Chesnavich, Multiple transition states in unimolecular reactions, J. Chem. Phys. 84 (1986) 2615–2619.
[18] J. Troe, V.G. Ushakov, A.A. Viggiano, On the model dependence of kinetic shifts in unimolecular reactions: the dissociation of the cations of benzene and n-butylbenzene, J. Phys. Chem. A 110 (2006) 1491–1499.
[19] T. Baer, Y. Li, Threshold photoelectron spectroscopy with velocity focusing: an ideal match for coincidence studies, Int. J. Mass Spectrom. 219 (2002) 381–389.
[20] B. Sztáray, T. Baer, The suppression of hot electrons in threshold photoelectron photoion coincidence spectroscopy using velocity focusing optics, Rev. Sci. Instrum. 74 (2003) 3763–3768.
[21] J.P. Kercher, W. Stevens, Z. Gengeliczki, T. Baer, Modeling ionic unimolecular dissociations from a temperature controlled TPEPCIO Study on 1-C_4H_9I ions, Int. J. Mass Spectrom. 267 (2007) 159–166.
[22] S. Borkar, B. Sztáray, Self-consistent heats of formation for the ethyl cation, ethyl bromide, and ethyl iodide from threshold photoelectron photoion coincidence spectroscopy, J. Phys. Chem. A 114 (2010) 6117–6123.
[23] K.D. Cook, J.W. Taylor, A Mass-spectrometric study of the effect of supersonic molecular-beam sampling on the clustering of acetic-acid vapor, Int. J. Mass Spectrom. Ion. Proc. 35 (1980) 259–271.
[24] L.A. Curtiss, K. Raghavachari, P.C. Redfern, V. Rassolov, J.A. Pople, Gaussian-3 (G3) theory for molecules containing first and second-row atoms, J. Chem. Phys. 109 (1998) 7764–7776.
[25] S.G. Lias Ionization Energy Data: http://webbook.nist.gov/chemistry/om/, 2006.
[26] Y.-R. Luo, Comprehensive Handbook of Chemical Bond Energies, CRC Press, Boca Raton, FL, 2007.
[27] N. Heinrich, H. Schwarz, On the role of ion dipole complexes in the isomerization dissociation reactions of ionized acetic-acid and its enol in the gas-phase—an abinitio molecular-orbital study, Int. J. Mass Spectrom. 79 (1987) 295–310.
[28] E. Murad, M.G. Inghram, Photoionization of aliphatic ketones, J. Chem. Phys. 40 (1964) 3263–3275.
[29] T. Baer, W.L. Hase, Unimolecular Reaction Dynamics: Theory and Experiments, Oxford University Press, New York, 1996.
[30] W.L. Hase, The criterion of minimum state density in unimolecular rate theory. An application to ethane dissociation, J. Chem. Phys. 64 (1976) 2442–2449.
[31] W. Stevens, B. Sztáray, N. Shuman, T. Baer, J. Troe, Specific rate constants $k(E)$ of the dissociation of the halobenzene ions: analysis by statistical unimolecular rate theories, J. Phys. Chem. A 113 (2009) 573–582.
[32] N.S. Shuman, M. Johnson, W.R. Stevens, M.E. Harding, J.F. Stanton, T. Baer, Tunneling in a simple bond scission: the surprising barrier in the H loss from $HCOOH^+$, J. Phys. Chem. A, in preparation.
[33] Y.J. Bomble, J. Vazquez, M. Kallay, C. Michauk, P.G. Szalay, A.G. Csaszar, J. Gauss, J.F. Stanton, High-accuracy extrapolated ab initio thermochemistry. II. Minor improvements to the protocol and a vital simplification, J. Chem. Phys. 125 (2006), 064108-1-064108/8.
[34] B. Ruscic, M. Schwarz, J. Berkowitz, Mechanisms of photodissociative ionization of HCOOH: the heat of formation of $COOH^+$, J. Chem. Phys. 91 (1989) 6772–6779.
[35] B.E. Miller, T. Baer, Kinetic energy release distribution in the fragmentation of energy selected vinyl and ethyl bromide ions, Chem. Phys. 85 (1984) 39–45.
[36] T. Shimanouchi, Tables of Molecular Vibrational Frequencies; Natl.Stand.Ref.Data.Ser.(NBS) # 39: U.S. Government Printing Office, Washington DC, 1972.
[37] M.E. Harding, J. Vazquez, B. Ruscic, A.K. Wilson, J. Gauss, J.F. Stanton, High-accuracy extrapolated ab initio thermochemistry. III. Additional improvements and overview, J. Chem. Phys. 128 (2008), 114111-1-114111/15.